thermal processes, as partially described in this paper.

Acknowledgment. This work is partially supported by a Grant-in-Aid for Special Project Research (No. 57119003) from the Ministry of Education, Science and Culture of Japan ("Design of Multiphase Biomedical Materials") and by scientific grants from the Asahi Glass Foundation for Industrial Technology, Toyoda Gosei Co., Ltd., and the Yokohama Rubber Co., Ltd.

References and Notes

(1) Hashimoto, T.; Kumaki, J.; Kawai, H. *Macromolecules* **1983**, 16, 641.
(2) Cahn, J. W. *J. Chem. Phys.* **1965**, *42*, 93.
(3) Dupplessix, R.; Picot, C.; Benoit, H. *J. Polym., Sci., Polym. Lett. Ed.* **1971**, *9*, 321.
(4) Flory, P. J. "Principles of Polymer Chemistry"; Cornell University Press: Ithaca, NY, 1967.
(5) Scott, R. L. *J. Chem. Phys.* **1949**, *17*, 268.
(6) Tompa, H. "Polymer Solutions"; Butterworths: London, 1956.
(7) Part 3: Sasaki, K.; Hashimoto, T. *Macromolecules*, following paper in this issue.
(8) χ values for the interaction of PS-Tol, PB-Tol, and PS-PB are 0.436, 0.465, and 0.10, respectively, according to Noolandi and Hong.[9]
(9) Noolandi, J.; Hong, K. M. *Ferroelectrics* **1980**, *30*, 117.
(10) Langer, J. S.; Bar-on, M.; Miller, H. D. *Phys. Rev. A* **1975**, *11*, 1417.
(11) Binder, K.; Stauffer, D. *Phys. Rev. Lett.* **1974**, *33*, 1006.
(12) Kawasaki, K.; Ohta, T. *Prog. Theor. Phys.* **1978**, *59*, 362.
(13) Lifshitz, I. M.; Slyozov, V. V. *J. Phys. Chem. Solids* **1961**, *19*, 35.
(14) Siggia, E. D. *Phys. Rev. A* **1979**, *20*, 595.
(15) Nojima, S.; Tsutsumi, K.; Nose, T. *Polym. J.* **1982**, *14*, 225.
(16) Kuwahara, N.; Tachikawa, M.; Hamano, K.; Kenmochi, Y. *Phys. Rev. A* **1982**, *25*, 3349.
(17) Snyder, H. L.; Meakin, P.; Reich, S. *J. Chem. Phys.* **1983**, *78* (6), 3334.
(18) Shimidzu, N.; Hashimoto, T.; Kawai, H., to be submitted to *Macromolecules* (part 4 of this series).
(19) Hashimoto, T.; Shibayama, M.; Kawai, H. *Macromolecules* **1983**, *16*, 1093.
(20) Shibayama, M.; Hashimoto, T.; Hasegawa, H.; Kawai, H. *Macromolecules* **1983**, *16*, 1427.
(21) Van Aartsen, J. J. *Eur. Polym. J.* **1970**, *6*, 919.
(22) Van Aartsen, J. J.; Smolders, C. A. *Eur. Polym. J.* **1970**, *6*, 1105.
(23) Feke, T.; Prins, W. *Macromolecules* **1974**, *7*, 527.
(24) The results presented here are consistent with the Cahn model but are also consistent with the Cook model,[25] a sort of modified Cahn model. The results may also be consistent qualitatively with Langer's model,[10] since in Langer's prediction the scattering maximum is only slowly varying.
(25) Cook, H. E. *Acta Metall.* **1970**, *18*, 297.
(26) Nish, T.; Wang, T. T.; Kwei, T. K. *Macromolecules* **1975**, *8*, 227.
(27) Snyder, H. L.; Meakin, P.; Reich, S. *Macromolecules* **1983**, *16*, 757.
(28) Gelles, R.; Frank, C. W. *Macromolecules* **1983**, *16*, 1448.
(29) It should be noted that eq 1 is valid for isolated spheres with monodisperse size distribution. In the case when the polydispersity exists in the size, eq 1 is only qualitatively true, and the rigorous value of $4\pi (R_s/\lambda) \sin (\theta_m/2)$ (R_s, average radius) depends on the distribution function for the particle size.
(30) One should note that the arguments similar to those in ref 29 must be applied on distribution of the periodicity D_s. The average periodicity D_s in real space will give only a qualitatively correct peak position in reciprocal space.

Time-Resolved Light Scattering Studies on the Kinetics of Phase Separation and Phase Dissolution of Polymer Blends. 3. Spinodal Decomposition of Ternary Mixtures of Polymer A, Polymer B, and Solvent

Kouji Sasaki† and Takeji Hashimoto*

Department of Polymer Chemistry, Faculty of Engineering, Kyoto University, Kyoto 606, Japan. *Received January 4, 1984*

ABSTRACT: An early stage of spinodal decomposition (SD) for the ternary mixtures of polystyrene (PS), polybutadiene (PB), and toluene (Tol) and of PS, polystyrene–polybutadiene diblock polymer (SB), and Tol was investigated by the time-resolved light scattering technique. The SD for the ternary systems in which Tol is a neutrally good solvent for all the polymers used in these studies was analyzed on the basis of the linearized theory of Cahn, coupled with a pseudobinary approximation and a mean-field approximation for the ternary solutions. An overall behavior in the early stage of SD seems to fit well, at least qualitatively, with the linearized theory coupled with the above two approximations. Quantitative deviations from the theory were observed, and they may be attributed to the validity of the special (mean field) model used for the ternary solutions and/or of the linearized theory, besides the experimental errors arising from difficulties studying the earliest stage of the process. The characteristic parameters describing the early stage of SD for the ternary systems were obtained in the context of the linearized theory and compared with those for the binary mixture of PS and poly(vinyl methyl ether).

I. Introduction

In the previous paper,[1] we found a spatial composition fluctuation with a characteristic periodicity which gives rise to a light scattering maximum for the films composed of binary and ternary mixtures of polystyrene (PS), polybutadiene (PB), and polystyrene–polybutadiene diblock polymers (SB) prepared by solvent casting with toluene (Tol), a neutrally good solvent for these polymers. These periodic fluctuations are found to develop and grow in the solutions during the phase separation due to spinodal decomposition (SD) and its subsequent coalescence processes.[2-14] The existence of SD and the coalescence processes were qualitatively demonstrated by a time-resolved laser light scattering technique using a silicone vidicon TV camera and VTR monitor system for the ternary systems composed of PS, PB, and Tol or PS, SB, and Tol.[1]

In the present paper we will focus our attention on the very early stage of SD for the ternary systems composed of PS/PB/Tol and PS/SB/Tol at critical and off-critical compositions. Section II describes the time-resolved light

†Present address: Toyoda Gosei Co., Ltd., 1, Nagahata, Ochiai, Haruhi-Mura, Nishikasugai-gun, Aichi-Prefecture 452, Japan.

0024-9297/84/2217-2818$01.50/0

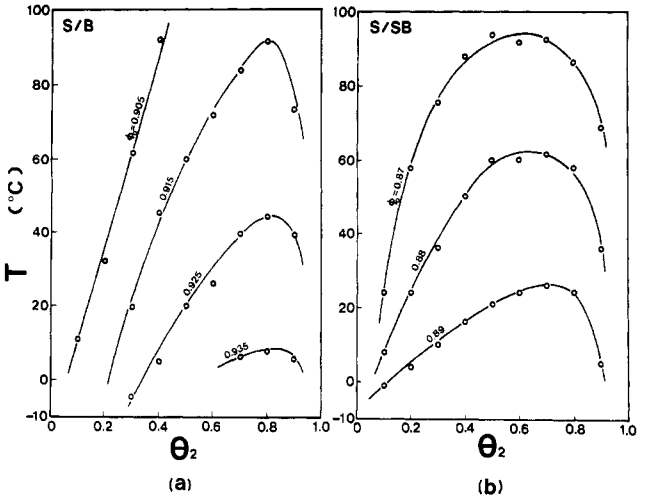

Figure 1. Cloud-point curves for (a) PS/PB/Tol and (b) PS/SB/Tol at various polymer volume fractions $(1 - \phi_0)$. θ_2 designates volume fractions of PB or SB in the polymer mixture, e.g., $\theta_2 = V_{PB}/(V_{PB} + V_{PS})$, where V_{PB} and V_{PS} are the volumes of PB and PS, respectively, and ϕ_0 designates volume fraction of solvent.

scattering data on the ternary mixtures in the early stage of SD. The data were analyzed on the basis of Cahn's linearized theory[2] of SD in the context of a *mean-field approximation*[15-18] coupled with a *pseudobinary* approximation [i.e., toluene primarily acts as a solvent which reduces polymer–polymer interaction (sections III and IV)]. The characteristic parameters describing the early stage of SD for the ternary systems were compared with those for a binary polymer mixtures of PS and poly(vinyl methyl ether) (PVME) (section VI).[13] A dramatic difference in time dependence of the scattering intensity in the SD regime and in the nucleation-growth regime[19] will be presented in section V.

II. Results

Figure 1 shows cloud-point curves for the ternary systems (a) PS/PB/Tol and (b) PS/SB/Tol in which ϕ_0 represents the volume fraction of solvent in the ternary mixture, and θ_2 is the volume fraction of PB or SB in the polymer mixture. The method used to evaluate the curves and the polymers used in these studies were described in detail in the previous paper.[1] PS, PB, and SB have number-average molecular weights of 151×10^3, 48×10^3, and 50×10^3, respectively, and heterogeneity indices $\bar{M}_w/\bar{M}_n$ of 1.41, 1.23, and 1.7, respectively. It was also pointed out in the paper that the composition $\theta_{2,c}$ at which the cloud point becomes maximum was not in good agreement with the critical composition predicted by a mean-field theory of Scott.[16]

In this paper the kinetics of phase separation was studied for off-critical mixture ($\theta_2 = 0.2$), designated as S/B-20, and near-critical mixture ($\theta_2 = 0.8$), designated as S/B-80, of PS/PB/Tol, and for near-critical mixture ($\theta_2 = 0.65$), designated as S/SB-65, of PS/SB/Tol as a function of quench depth $\Delta T = T_x - T_{cl}$, where T_x and T_{cl} are the temperatures of isothermal phase separation and of the cloud point, respectively. The polymer concentrations $(1 - \phi_0)$ studied in this work are fixed, $\phi_p = 1 - \phi_0 = 0.075$ for S/B-80, 0.095 for S/B-20, and 0.115 for S/SB-65, and corresponding cloud points are 46.5, 43.0, and 42.0 °C for S/B-80, S/B-20, and S/SB-65, respectively.

Figure 2 schematically illustrates a pseudobinary approximation on the phase separation of the ternary systems. Since Flory interaction parameters[15] between PS and Tol (χ_{PS-Tol}) and PB and Tol (χ_{PB-Tol}) are about the same, the solvent (Tol) is equally partitioned in the PS and

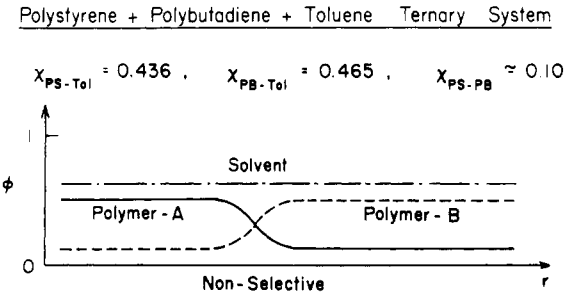

Figure 2. Pseudobinary approximation of the ternary system A/B/S (S designating a neutrally good solvent for the polymers A and B).

PB (or SB) phases, giving rise to a phase separation between PS solution and PB (or SB) solution which will be called here as *pseudobinary* phase separation. The solvent will primarily act as a diluent to decrease the interaction parameter between PS and PB (or Sb), χ_{PS-PB}. The ternary system with SB generally involves two kinds of phase separations: (i) phase separation between PB and SB solutions (polymer–polymer liquid–liquid phase separation) and (ii) "microphase separation" of SB diblock polymers. It was indicated previously[1] that the microphase separation of SB will not occur at polymer concentrations covered in this work, even after completion of the macroscopic phase separation of PS and SB solutions as discussed briefly in the previous paper.[1] Only polymer–polymer phase separation occurs even for PS/SB/Tol. Consequently, incorporation of polystyrene block in SB does not complicate the polymer–polymer phase separation but essentially weakens the χ parameter between the constituent polymers. As the total polymer concentration increases, the microphase separation begins to occur as a consequence of the concentration fluctuations built up by the polymer–polymer phase separation. When concentration of the SB in the SB-rich phase exceeds the concentration at which the microphase separation occurs, the SB starts to undergo the microphase separation, resulting in unique multiphase structures. This is a new regime, the studies of which are beyond the scope of the present paper but are believed to be important from both academic and industrial points of view.

The kinetics of the phase separation was observed by a time-resolved light scattering technique in which the change of scattering intensity curves was observed as a function of time and scattering vector q after temperature drops from 50 °C to T_x, 50 °C being higher than T_{cl}'s of the solution

$$q = (4\pi/\lambda) \sin(\theta/2) \qquad \text{(II-1)}$$

where θ and λ are the scattering angle and wavelength of the light in the medium, respectively. The sample cell and a method of temperature drop were described in the previous paper.[1] In the previous paper, the changes of the scattering profiles followed by the initiation of the phase separation were qualitatively detected by silicone vidicon and VTR monitor systems. Here the phase-separation kinetics was detected more quantitatively by scanning a photomultiplier, a brief description of which was given elsewhere.[13]

Figure 3 shows a typical change of scattering profiles with time after insertion of the sample cell, initially at 50 °C which is above T_{cl}, into the metal block controlled at $T_x = 43.5$ °C ($\Delta T = -3.0$ °C) for S/B-80 with $\phi_0 = 0.925$. The scattering profiles were reconstructed from the plots of scattered intensity vs. time at various q's such as shown in Figure 4 and correspond to those at each time slicing.

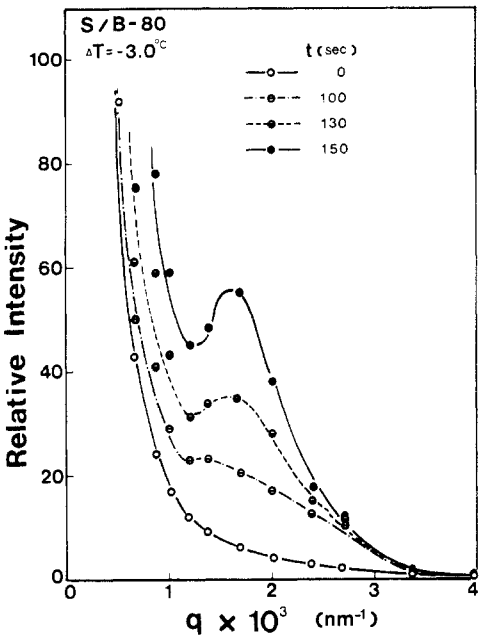

Figure 3. Typical change of the light scattering profile with time after insertion of the sample cell into the metal block controlled at the phase-separation temperature T_x for the S/B-80 at ϕ_0 = 0.925 and ΔT = -3.0 °C, $\Delta T = T_x - T_{cl}$ (T_{cl} = 46.5 °C).

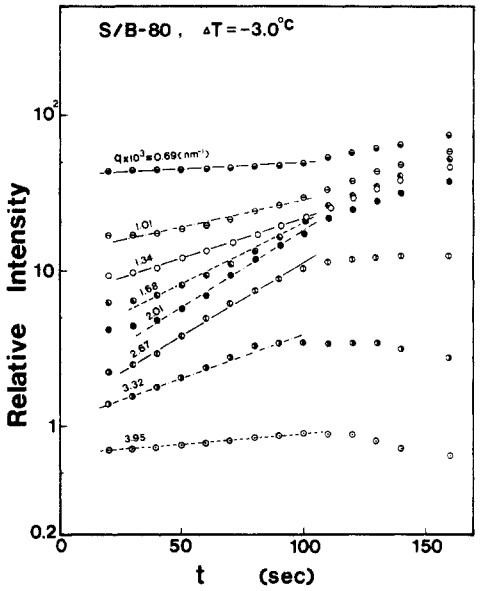

Figure 4. Typical variation of the scattered intensity with time during the phase separation for the S/B-80 at ϕ_0 = 0.925 and ΔT = -3.0 °C.

It should be noted that time t always refers to the *time after insertion of the sample cell* into the metal block at T_x throughout this paper and that the temperature change from the initial temperature T_i (50 °C in this case) to T_x was characterized by a exponential function

$$T(t) = (T_i - T_x) \exp(-t/\tau) + T_x \qquad \text{(II-2)}$$

with *relaxation time* τ of 9.8 s. It is clearly seen that the scattering maximum appears at $q_m \cong 2 \times 10^{-3}$ nm^{-1} after initiation of the phase separation. The scattering intensity increases but the scattering vector q_m of maximum intensity does not significantly change with time, the tendencies of which are in accord qualitatively with observation with a silicone vidicon–VTR apparatus as described in the previous paper[1] and qualitatively with a theoretical prediction given by Cahn's linearlized theory of spinodal decomposition.[2]

The changes of the scattered intensity at various q's with time t were plotted in Figure 4 where logarithms of the intensity were plotted against a linear scale of t. It is clearly seen that the scattered intensity exponentially increases with time t in the early stage of phase separation ($t \lesssim 100$ s), in accord with theoretical prediction of Cahn on spinodal decomposition.[2]

$$I(q,t) = I(q, t = 0) \exp[2R(q)t] \qquad \text{(II-3)}$$

From the slope, one can measure the *relaxation rate* (or *growth rate*) of the intensity $2R(q)$ or that of concentration fluctuation $R(q)$ with a particular wavenumber q as defined by $2\pi/\Lambda$ where Λ is the wavelength or identity period of the concentration fluctuations.

$$q = 2\pi/\Lambda = (4\pi/\lambda) \sin(\theta/2) \qquad \text{(II-4)}$$

$R(q)$ is a function of q (i.e., a function of $2\pi/\Lambda$ in real space and of scattering vector in reciprocal space), increasing with q to reach a maximum value at particular q and then decreasing with a further increase of q. In the later stage of spinodal decomposition ($t \gtrsim 100$ s), the intensity change with time deviates from the exponential behavior as described by eq II-3, which is due to onset of coarsening processes.[3-7,11,12,14] Although the studies on the later stage are interesting research projects, they are beyond the scope of the present paper.

It should be noted that Figure 4 shows nonexponential behavior even during the earliest stages of the phase separation where one would expect a best fit of the exponential behavior with Cahn's prediction. This nonexponential behavior is best interpreted as a consequence of a finite time required for the temperature jump. From eq II-2 with τ = 9.8 s, one would expect that achievements of $(T(t) - T_x)/(T_i - T_x) = 0.1$ and 0.05 require t = 23 and 39 s, respectively. This approximately corresponds to the time region where the discrepancy from the nonexponential behavior is found.

III. Analyses Based on Linearized Theory of Spinodal Decomposition

In this section we will analyze our data on the ternary systems on the basis of Cahn's linearized theory of spinodal decomposition, developed for the incompressible binary mixtures.[2] The analyses will be made in the context of the *pseudobinary approximation*.

Cahn[2] predicted that a growth of spatial concentration fluctuation of a particular component during the early stage of spinodal decomposition is given by

$$\Delta c(\mathbf{r}) = \sum_{\mathbf{q}} \exp[R(q)t]\{A(q) \cos(\mathbf{q}\cdot\mathbf{r}) + B(q) \sin(\mathbf{q}\cdot\mathbf{r})\} \qquad \text{(III-1)}$$

for an isotropic growth where $R(q)$ is growth rate of the fluctuations with wavenumber $q = 2\pi/\Lambda$ and is given by

$$R(q) = Mq^2\{-(\partial^2 f/\partial c^2) - 2\kappa q^2\} \qquad \text{(III-2)}$$

where f is the free energy density of homogeneous system in which the composition of one component is given by a constant value c everywhere in the space, and κ is the coefficient describing the excess free energy density associated with composition gradient $(\kappa(\nabla c)^2)$.[2,19] Equations III-1 and III-2 were obtained by neglecting nonlinear terms in the modified diffusion equation

$$\partial c/\partial t = M[(\partial^2 f/\partial c^2)\nabla^2 c - 2\kappa\nabla^4 c + (\text{nonlinear terms})] \qquad \text{(III-3)}$$

where M is the classical mobility constant. The linearized theory leading to eq III-1 and III-2 predicts time dependence of the elastic scattered intensity of light, X-ray, and

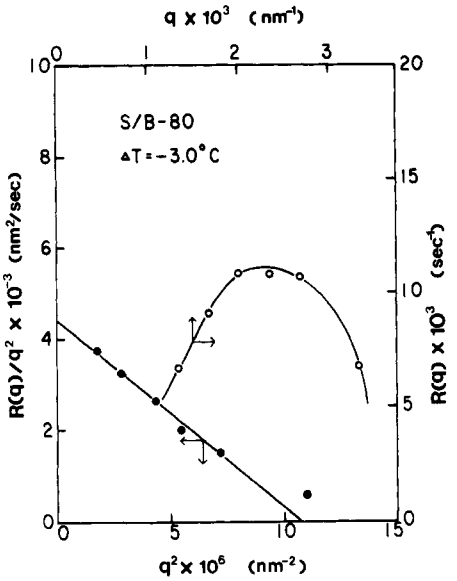

Figure 5. Analyses of the early stage of the spinodal decomposition, based on Cahn's linearized theory for S/B-80 at ϕ_0 = 0.925 and ΔT = -3.0 °C.

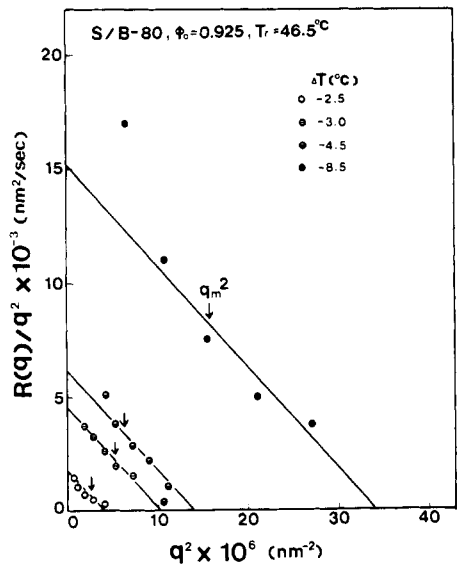

Figure 6. Analyses of the early stage of the spinodal decomposition, based on Cahn's linearized theory for S/B-80 at ϕ_0 = 0.925 and various quench depths ΔT.

neutron scattering during the spinodal decomposition as given by eq II-3.

Equation III-2 predicts that a particular mode of concentration fluctuations with wavenumber q_m can have maximum growth rate $R(q_m)$.

$$q_m^2 = -(\partial^2 f/\partial c^2)/(4\kappa) \quad \text{(III-4)}$$

$$R(q_m) = M(\partial^2 f/\partial c^2)^2/(8\kappa) \quad \text{(III-5)}$$

The existence of the wavenumber q_m results from two opposing physical factors: (1) one associated with *transport property* giving $R(q) \sim Mq^2$, i.e., the greater the q value, the shorter the distance over which the molecules are required to translate to build up the fluctuations, and hence the faster the growth rate, and (2) the other associated with *thermodynamic property*, giving $R(q) \sim (\alpha - \beta q^2)$ (α and β should be essentially independent of q), i.e., the larger the q, the greater the gradient free energy of the fluctuations, and hence the slower the growth rate. It should be noted that the most probable wavenumber of the fluctuations q_m is purely determined by thermodynamic conditions such as quench depth but that the maximum growth rate $R(q_m)$ depends on the transport property as well.

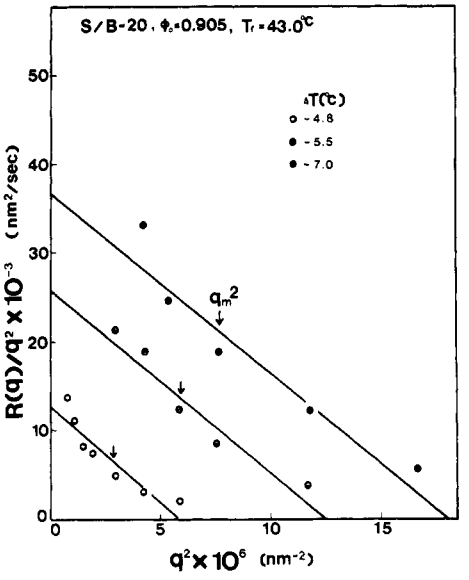

Figure 7. Analyses of the early stage of the spinodal decomposition, based on Cahn's linearized theory for S/B-20 at ϕ_0 = 0.905 and various quench depths ΔT.

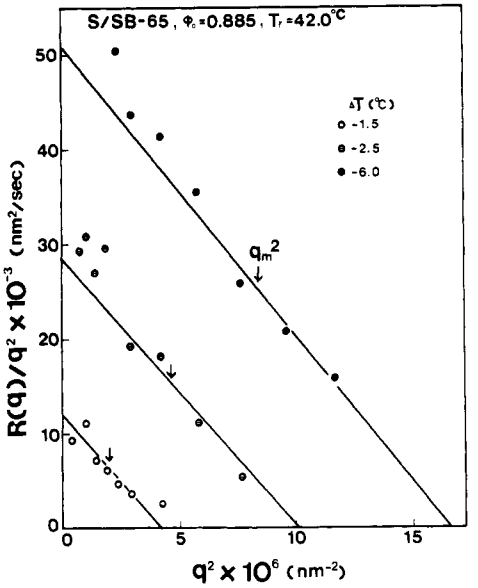

Figure 8. Analyses of the early stage of the spinodal decomposition, based on Cahn's linearized theory for S/SB-65 at ϕ_0 = 0.885 and various quench depths ΔT.

Figure 5 shows the experimental test of eq III-2 for S/B-80, ϕ_0 = 0.925 and at ΔT = -3.0 °C (near-critical mixture) where $R(q)/q^2$ and $R(q)$ are plotted as function of q^2 and q, respectively. It is clearly shown that the early stage of SD ($t \lesssim 100$ s for this particular case, see Figure 4) can be well described, at least qualitatively, by the linearized theory of Cahn.[2] One should note that there exist quantitative deviations of the experimental results from the theory of Cahn. From the q dependence of $R(q)$ in Figure 5, $q_m \simeq 2.3 \times 10^3$ nm^{-1}, and hence one would expect $q_c = q_m 2^{1/2} \simeq 3.25 \times 10^3$ nm^{-1}. However $R(q)$ is not zero at $q > q_c$ as seen in Figure 4 (see intensity increase at q = 3.32 and 3.95) and in Figure 5. This discrepancy may illustrate quantitative failure of the theory.

Equation III-2 was further tested for various ternary mixtures as a function of quench depth ΔT, the results of which were shown in Figure 6 for S/B-80 at ϕ_0 = 0.925,

Figure 7 for S/B-20 at ϕ_0 and 0.905, and Figure 8 for S/SB-65 at $\phi_0 = 0.885$. Overall and qualitative fits of the experimental data with the linearized theory seem to be good, though there are quantitative deviations from the straight lines in the plots of $R(q)/q^2$ vs. q^2, as may be seen in curvature in the majority of the plots, especially for the data obtained for a large quench depth, ΔT. It may be further pointed out that this curvature is similar to the curvature observed in all other systems studied and has been used by all other workers in the field to claim failure of the linearized theory. At present we feel that this point deserves further study particularly for polymeric systems, because they could have much a slower growth rate $R(q)$ than the rates encountered in this study, depending on molecular weights and concentrations. Hence they would provide ideal model systems for further careful, rigorous, and quantitative studies of the early stages. We present below further qualitative analyses in the context of the linearized theory.

From the intercepts of $R(q)/q^2$ at $q = 0$, one can estimate the *apparent diffusion coefficient*, D_{app}, as defined by

$$D_{app} \equiv \left.\frac{R(q)}{q^2}\right|_{q=0} = -M\left(\frac{\partial^2 f}{\partial c^2}\right)V \qquad \text{(III-6)}$$

where V is the total volume of the systems. It should be noted that the greater the value of D_{app} the larger the curvature of $R(q)$ with q at $q = q_m$, and hence the sharper the maximum of $R(q)$ at $q = q_m$, since

$$D_{app} = \frac{1}{8}\left.\frac{\partial^2 R(q)}{\partial q^2}\right|_{q=q_m} \qquad \text{(III-7)}$$

Thus the greater the quench depth, the better defined is the spinodal ring, i.e., the scattering maximum arising from periodic concentration fluctuations. This tendency was experimentally confirmed. D_{app} decreases with decreasing quench depth ΔT as found in these figures and should vanish at spinodal temperature T_s, since $(\partial^2 f/\partial c^2) = 0$ at $T = T_s$.

From the plots of $R(q)/q^2$ vs. q^2 one can also estimate q_m since

$$q_m^2 = q_c^2/2 \qquad \text{(III-8)}$$

and

$$R(q = q_c) = 0 \qquad \text{(III-9)}$$

where q_c is called as the maximum wvenumber of the fluctuations which can grow. The arrows in the figures indicate q_m^2, which again decreases with decreasing quench depth $|\Delta T|$ and should go to zero at $T = T_s$. It should be pointed out that q_m's thus estimated agree with the values estimated directly from $R(q)$ vs. q within the experimental errors.[24]

The slopes of the straight lines in the plot of $R(q)/q^2$ vs. q^2 are nearly independent of ΔT for each ternary system.

These characteristic parameters D_{app}, q_m, $\varkappa D_c$, and $R(q_m)$ describing an early stage of spinodal decomposition will be further analyzed in the next section in the context of mean-field approximation.[18]

IV. Further Analyses Based on a Special (Mean-Field) Model for the Solutions

In order to understand molecular parameters affecting $-(\partial^2 f/\partial c^2)$ and $\varkappa$, one needs a specific model relevant to polymer mixtures. Here we adopt a formalism proposed by de Gennes for incompressible, binary liquids composed of macromolecules.[18] As briefly reviewed in the previous paper,[1] de Gennes expressed the free energy density of homogeneous mixture $f(c)$ by the Flory–Huggins formula in the context of *mean-field approximation*.[15-17] In describing the gradient free energy terms $(\nabla c)^2$ etc., he also employed a *linearization approximation* and took into account "*entropy effect*" of local variation in c which arises from "connectivity" of monomeric units.[18] The energetic contribution to the gradient term, associated with the finite range of energetic interaction of monomer units,[2] was neglected as it is generally small compared with the entropic contribution.[18]

On the basis of the approximations as described above, $R(q)$ was given by

$$R(q) = q^2\Lambda(q)\left\{2\chi - \frac{1}{Nc(1-c)} - \frac{a^2}{36c(1-c)}q^2\right\} \qquad \text{(IV-1)}$$

where $\Lambda(q)$ is the q-dependent Onsager coefficient given, on the basis of the scaling argument[18] by

$$\Lambda(q) = Nc(1-c)D_c \qquad \text{for } qR_0 \ll 1 \qquad \text{(IV-2)}$$

in the small q regime (R_0 being the unperturbed end-to-end distance of polymer coil).[25] The Onsager coefficient $\Lambda(q \to 0)$ is related to the classical mobility constant M in the Cahn theory

$$M = \Lambda(q \to 0)/k_BT \qquad \text{(IV-3)}$$

where k_BT is the Boltzmann energy. The quantities $-(\partial^2 f/\partial c^2)$ and $\varkappa$ in the theory of Cahn are now given by[27]

$$-\left(\frac{\partial^2 f}{\partial c^2}\right) = (\text{const})\left(\frac{\chi - \chi_s}{\chi_s}\right) \qquad \text{(IV-4)}$$

$$\varkappa = (\text{const})R_0^2/72 \qquad \text{(IV-5)}$$

where

$$(\text{const}) = \frac{k_BT}{V}\frac{1}{Nc(1-c)} \qquad \text{(IV-6)}$$

N is the degree of polymerization of polymer A and B. The two polymers were assumed to have identical degree of polymerizations, identical diffusion constants D_c, and identical Kuhn statistical segment lengths a. χ_s is the χ parameter at spinodal point T_s.

$$\chi_s^{-1} = 2Nc(1-c) \qquad \text{(IV-7)}$$

The SD at the small q regime should occur as a consequence of translational diffusion of polymer coils through "reptation".[20,21] Since the mechanism of SD in the polymeric systems in this regime is the same as that in the small molecular systems, $R(q)$ should have the same functional form as that given by eq III-2. In fact from eq IV-1, and IV-4 to IV-6, it follows that

$$R(q) = q^2D_c\left[\left(\frac{\chi - \chi_s}{\chi_s}\right) - \left(\frac{R_0^2}{36}\right)q^2\right] \qquad \text{(IV-8)}$$

It may be pointed out that the deviation from the special (mean field) theory for the ternary solutions might alter q dependence of $R(q)$, simply because it changes the term associated with the thermodynamic properties, i.e., $[(\chi - \chi_s)/\chi_s - (R_0^2/36)q^2]$. The deviation, however, will not change the term associated with transport property, i.e., q^2D_c. Thus the deviation of the data points from the straight line in the plot $R(q)/q^2$ vs. q^2 may also result from the deviation from the special mean-field approximation for the ternary solutions.

In the *pseudobinary approximation*, we further assume that D_c, χ, χ_s and R_0 are the corresponding values in the presence of neutrally good solvent. It should be noted that

Table I
Characteristic Parameters for the Early Stage of Spinodal Decomposition of the Ternary Systems

	$q_m^2/\Delta T$, $cm^{-2}/°C$	$D_{app}/\Delta T$, $(cm^2\ s^{-1})/°C$	$R(q_m)^{1/2}/\Delta T$, $s^{-1/2}/°C$	$\Lambda_m/\Delta T^{-1/2}$,[a] $cm/°C^{-1/2}$	$\tau_m/\Delta T^{-2}$,[b] $s/°C^{-2}$
S/B-20	1.8×10^8	8.9×10^{-11}	10×10^{-2}	4.7×10^{-4}	1.0×10^2
S/B-80	2.0×10^8	1.9×10^{-11}	4.2×10^{-2}	4.4×10^{-4}	5.7×10^2
S/SB-65	1.4×10^8	8.0×10^{-11}	7.4×10^{-2}	5.3×10^{-4}	1.8×10^2
cf. PS/PVMe[c] (SE-70)	$(107 \pm 50) \times 10^8$	5.5×10^{-13}	$(5.5 \pm 1) \times 10^{-2}$	$(0.6 \pm 0.1) \times 10^{-4}$	$(3.0 \pm 1) \times 10^2$

[a] $\Lambda_m = 2\pi/q_m \sim \Delta T^{-1/2}$. [b] $\tau_m = 1/R(q_m) \sim \Delta T^{-2}$. [c] Hashimoto, T.; et al. *Macromolecules* **1983**, *16*, 641.

D_c becomes very large, χ and χ_s become small, and R_0 becomes slightly large in the presence of the solvent. Thus in the context of mean-field approximation, the characteristic parameters describing early stage of SD are given by

$$D_{app} = D_c \frac{\chi - \chi_s}{\chi_s} \qquad \text{(IV-9)}$$

$$q_m^2 = (1/2)q_c^2 = \frac{18}{R_0^2} \frac{\chi - \chi_s}{\chi_s} \qquad \text{(IV-10)}$$

$$R(q_m)^{1/2} = \frac{3D_c^{1/2}}{R_0} \frac{\chi - \chi_s}{\chi_s} \qquad \text{(IV-11)}$$

and the slope of the plot $R(q)/q^2$ vs. q^2 is given by

$$|\text{slope}| = 2D_c\varkappa = (\text{const})\frac{1}{36}R_0^2 D_c \qquad \text{(IV-12)}$$

Expanding χ into a series about $T = T_s$

$$\chi(T) = \chi(T_s) + \left(\frac{\partial\chi}{\partial T}\right)_{T_s}(T - T_s) + \ldots \qquad \text{(IV-13)}$$

one obtains[1]

$$\frac{\chi - \chi_s}{\chi_s} = \left(\frac{\partial \ln \chi}{\partial T}\right)_{T_s}(T - T_s) + \ldots \qquad \text{(IV-14)}$$

Thus q_m^2, D_{app}, and $R(q_m)^{1/2}$ should be proportional to the quench depth $\Delta T = T - T_s = T_x - T_s$. It should be noted that for the UCST systems, $(\partial \ln \chi/\partial T)_{T_s} < 0$, and $\Delta T < 0$, and hence $(\chi - \chi_s)/\chi_s > 0$, and that, for the narrow temperature range of interests as characterized by variation of quench depth over a few degrees Celsius, D_c and R_0 should be almost independent of temperature. Thus the |slope| in eq IV-8 should be independent of ΔT.

The predictions as described above on the basis of the mean-field approximation were critically tested in Figures 9–12.[23] It is clearly shown, within experimental errors, that q_m^2, D_{app} (intercept in Figure 10), and $R(q_m)^{1/2}$ are linearly proportional to the quench depth $|\Delta T|$ for all the systems studied in this work[28] and that the slope is independent of $|\Delta T|$, as predicted from the theory. The results obtained from these figures are summarized in Table I and compared with those previously obtained for binary polymer mixture of PS and poly(vinyl methyl ether) (PVME) also on the early stage of SD in the context of the mean-field approximation.[1]

From Figure 9, q_m^2 is proportional to quench depth $|\Delta T|$, and q_m^2 per unit quench depth was shown to be about $(1.5–2) \times 10^8$ $cm^{-2}/°C$ for all the three samples. The equality of $q_m^2/\Delta T$ for these samples suggests that the values $(1/R_0^2)(\partial \ln \chi/\partial T)_{T_s}$ are about the same for these samples. Since $q_m^2 \sim \Delta T$, $\Lambda_m = 2\pi/q_m \sim \Delta T^{-1/2}$. The value $\Lambda_m/\Delta T^{-1/2}$ is about 4–5 $\mu m/°C^{-1/2}$ for all the samples.

The apparent diffusivity per unit quench depth, $D_{app}/\Delta T$, is in the range from 2×10^{-11} to 10×10^{-11} $cm^2/(s\ °C)$. The variations of the values with samples depend on $D_c(\partial \ln \chi/\partial T)_{T_s}$.

The value $R(q_m)^{1/2}/\Delta T$ is in the range of about (5–10) $\times 10^{-2}$ $s^{-1/2}/°C$, the variation of which should depend on $(D_c^{1/2}/R_0)(\partial \ln \chi/\partial T)_{T_s}$ and be predicted from variation of R_0, D_c, and $(\partial \ln \chi/\partial T)_{T_s}$ with the samples. Such de-

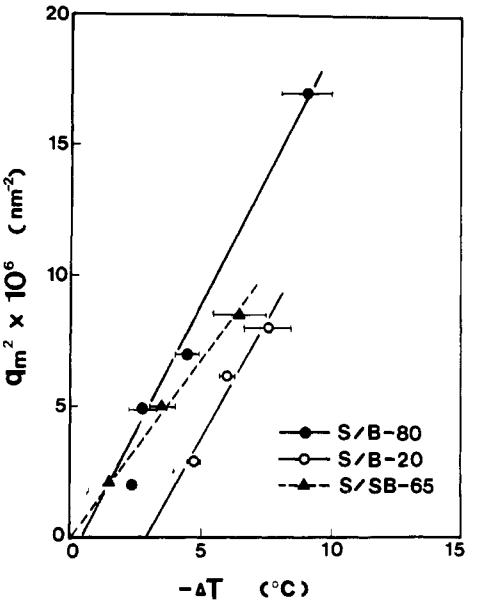

Figure 9. Plot of q_m^2 as a function of quench depth $-\Delta T$. The analysis is based on the linearized theory of SD and mean-field approximation.

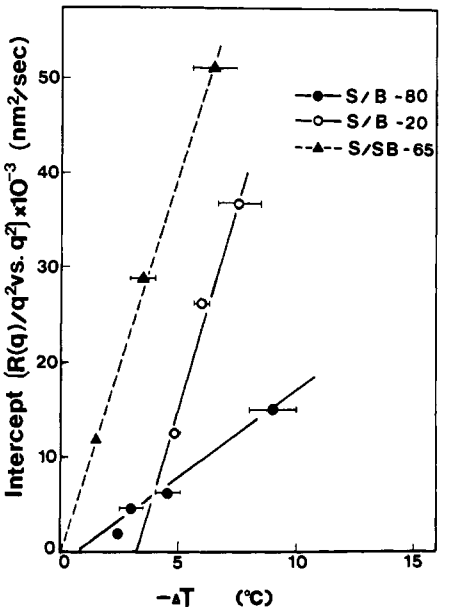

Figure 10. Plot of the apparent diffusivity D_{app} (intercept of the plot of $R(q)/q^2$ vs. q^2 at $q = 0$) as a function of quench depth $-\Delta T$. The analysis is based on the linearized theory of SD and mean-field approximation.

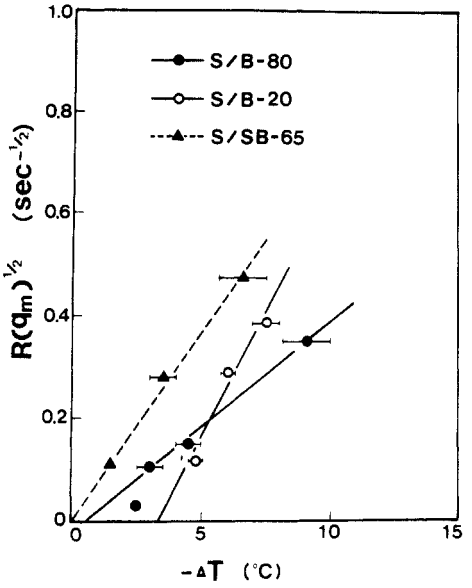

Figure 11. Plot of $R(q_m)^{1/2}$ as a function of the quench depth $-\Delta T$. The analysis is based on the linearized theory of SD and mean-field approximation.

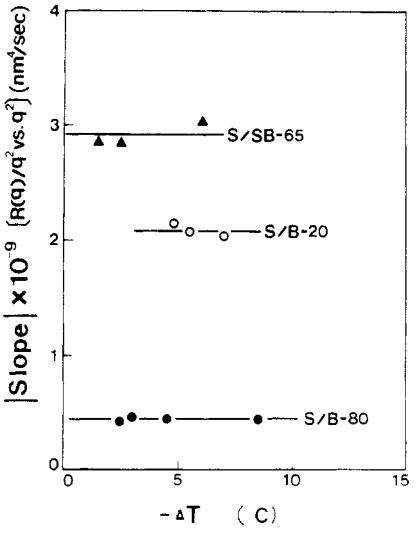

Figure 12. Absolute value of the slope in the plot of $R(q)/q^2$ vs. q^2 as a function of quench depth $-\Delta T$.

tailed discussions, however, are beyond the scope of the present studies. Since $R(q_m)^{1/2}$ is proportional to ΔT, the relaxation time $\tau_m = 1/R(q_m)$ should be proportional to ΔT^{-2}. The value τ_m per unit ΔT^{-2} is on the order of 10^2 s/°C^{-2}. If ΔT is increased by 1 order of magnitude from 1 to 10 °C, τ_m is decreased by 2 orders of magnitude from 100 to 1 s.

From the results and discussions made in sections III and IV it may be concluded that the overall picture in the early stage of spinodal decomposition of the ternary systems can be described approximately by the linearized theory based on the pseudobinary approximation.

The ternary systems as designated by S/B-80 and S/SB-65 have nearly critical compositions, while the system S/B-20 has off-critical composition, as shown in Figure 1. At the spinodal point $(\chi - \chi_s)/\chi_s = 0$ and hence q_m^2, D_{app}, and $R(q_m)^{1/2}$ should become zero. This principle provides a dynamic method to determine the spinodal phase boundary. It is clearly seen in Figures 9–11 that q_m^2, D_{app}, and $R(q_m)^{1/2}$ become zero at $\Delta T = 0$, and hence T_s is nearly equal to T_{cl}, cloud point for the near critical mixtures. However for the off-critical mixture S/B-20, they become zero at $\Delta T \sim -3$ °C, and hence T_s lies 3 °C below the cloud

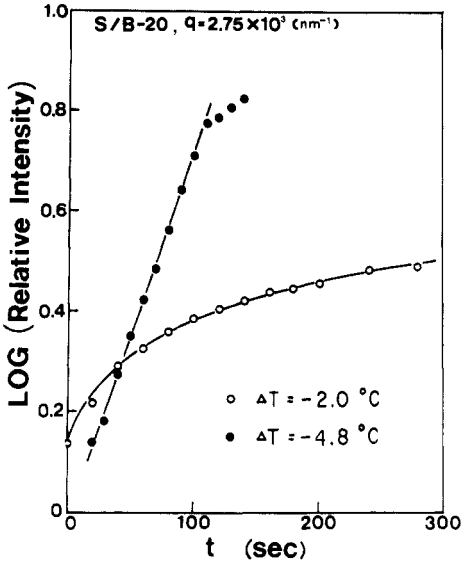

Figure 13. Typical variation of the scattered intensity with time during the phase separation according to the spinodal decomposition ($\Delta T = -4.8$ °C, solid circles) and nucleation-growth ($\Delta T = -2.0$ °C, open circles) for S/B-20 at $\phi_0 = 0.925$.

point, the conclusion of which is further confirmed in next section.

V. Scattering Behavior in the Nucleation-Growth Regime as Compared with That in the Spinodal-Decomposition Regime

For the off-critical mixture S/B-20 the phase separation should occur according to nucleation-growth (NG) mechanism if the quench depth $|\Delta T|$ is smaller than 3 °C. It was shown in the previous paper[1] that the phase separation in NG regime does not give scattering maximum as in the case of SD but gives the scattering patterns in which the intensity montonically decreases with an increase in the scattering angle. The scattered intensity itself increases with time during the course of the phase separation.

Figure 13 shows a typical intensity change at the particular scattering vector q with time after intiation of the phase separation for the off-critical mixture. The figure includes the intensity change for the phase separation in SD regime (i.e., the case of $\Delta T = -4.8$ °C, solid circles) as well as that for the phase separation in NG regime (i.e., the case of $\Delta T = -2.0$ °C, open circles). In the early stage of SD, the intensity exponentially increases with time, but in the phase separation according to NG, the intensity does not increases exponentially from the very beginning of the phase separation. Thus the scattering behavior and time dependence of the scattered intensity are spectacularly different, depending on the mechanism of the phase separation for the particular ternary systems studied here, which can be used to characterize the mechanism of the phase separation.

VI. Comparisons with the Binary Polymer–Polymer Mixture

Here we shall compare the characteristic parameters characterizing the early stage of SD of the ternary systems with those of a binary mixture of PS/PVME reported in the previous paper,[13] again in the context of mean-field approximation. Here we shall be concerned only with order-of-magnitude type arguments.

The characteristic parameters for the binary system of PS/PVME are also summarized in Table I. PS used in PS/PVME mixture was identical with the PS used in the ternary mixtures. The number-average molecular weight

and the heterogeneity index ($\bar{M}_w/\bar{M}_n$) of PVME were 4.6 $\times 10^4$ and 2.7, respectively, which are roughly identical with those of PB and SB used in the ternary mixtures. Therefore R_0's in eq IV-10 and IV-11 for the ternary and binary systems are roughly identical with each other.

The value $q_m^2/\Delta T$ for the binary mixture is about 1–2 orders of magnitude greater than that for the ternary mixture. According to eq IV-10 and IV-14 this implies that the absolute value of $(\partial \ln \chi/\partial T)_{T_s}$ for PS/PVME is greater than that for the ternary systems by the same order of magnitude, since R_0 itself is about the same for the binary and ternary systems. This is an interesting finding in regard to temperature dependence of χ parameter at spinodal points for the LCST and UCST systems. It would be even more interesting if the temperature coefficients of χ at LCST and UCST were measured for the same sample. It should be noted that the PS/PVME system has positive $(\partial \ln \chi/\partial T)_{T_s}$ and ΔT since it has LCST. The value $\Lambda_m/\Delta T^{-1/2}$ for the PS/PVME system is smaller than that for the ternary systems by about an order of magnitude, as is predictable from $q_m^2/\Delta T$.

The apparent diffusivity per unit quench depth, $D_{app}/\Delta T$, for the PS/PVME system is 2 orders of magnitude smaller than that for the ternary systems. This implies that $D_c(\partial \ln \chi/\partial T)_{T_s}$ for the PS/PVME system is 2 orders of magnitude smaller than that for the ternary systems. With information obtained on $(\partial \ln \chi/\partial T)_{T_s}$ from $q_m^2/\Delta T$, D_c for the PS/PVME is found to be about 3 orders of magnitude smaller than that for the ternary systems. Since molecular weights of component polymers are about the same for the two systems, this difference may be attributed to concentration dependence of D_c. Scaling theory predicts that at high concentrations (where the "concentration-blob" size approaches the "temperature-blob" size so that polymer chains become in Θ state) D_c scale as[21,22]

$$D_c \sim \phi_p^{-3} \qquad \text{(VI-1)}$$

where ϕ_p is the polymer concentration. Since $\phi_p \sim 0.1$ for the ternary systems, the concentration dependence of D_c can account for the observed difference in the values of D_c's.

The value $R(q_m)^{1/2}/\Delta T$ for the PS/PVME is about the same as that for the ternary systems, which can be interpreted as the values $D_c^{1/2}(\partial \ln \chi/\partial T)_{T_s}$ being about the same for all the systems from eq IV-11 and IV-14. More precisely, the effect of the PS/PVME system having a larger value of $(\partial \ln \chi/\partial T)_{T_s}$ (1–2 orders of magnitude larger than the ternary systems) was counterbalanced by the effect of the system having a lower value of D_c (3 orders of magnitude less). The relaxation times τ_m for the fluctuations to grow are also about the same for all the systems, as will be predictable from the values $R(q_m)^{1/2}/\Delta T$.

Acknowledgment. This work is partially supported by a scientific grant from the Asahi Glass Foundation for Industrial Technology. We are grateful to Prof. H. Kawai for his encouragement of this work.

References and Notes

(1) Part 2: Hashimoto, T.; Sasaki, K.; Kawai, H., *Macromolecules*, preceding paper in this issue.
(2) Cahn, J. W. *J. Chem. Phys.* **1965**, *42*, 93.
(3) Langer, J. S.; Bar-on, M.; Miller, H. D. *Phys. Rev. A* **1975**, *11*, 1417.
(4) Binder, K.; Stauffer, D. *Phys. Rev. Lett.* **1974**, *33*, 1006.
(5) Kawasaki, K.; Ohta, T. *Prog. Theor. Phys.* **1978**, *59*, 362.
(6) Lifshitz, I. M.; Slyozov, V. V. *J. Phys. Chem. Solids* **1961**, *19*, 35.
(7) Siggia, E. D. *Phys. Rev. A* **1976**, *A20*, 595.
(8) van Aartsen, J. J. *Eur. Polym. J.* **1970**, *6*, 919.
(9) van Aartsen, J. J.; Smolders, C. A. *Eur. Polym. J.* **1970**, *6*, 1105.
(10) Feke, T.; Prins, W. *Macromolecules* **1974**, *7*, 527.
(11) Nojima, S.; Tsutsumi, K.; Nose, T. *Polym. J.* **1982**, *14*, 225.
(12) Kuwahara, N.; Tachikawa, M.; Hamano, K; Kenmochi, Y. *Phys. Rev. A* **1982**, *A25*, 3349.
(13) Hashimoto, T.; Kumaki, J.; Kawai, H. *Macromolecules* **1983**, *16*, 641 (part 1 of this series).
(14) Snyder, H. L.; Meakin, P. L.; Reich, S. *Macromolecules* **1983**, *16*, 757.
(15) Flory, P. J. "Principles of Polymer Chemistry", Cornell University Press: Ithaca, NY, 1967.
(16) Scott, R. L. *J. Chem. Phys.* **1949**, *17*, 268.
(17) Tompa, H. "Polymer Solutions"; Butterworths: London, 1956.
(18) de Gennes, P.-G. *J. Chem. Phys.* **1980**, *72*, 4756.
(19) Cahn, J. W.; Hilliard, J. E. *J. Chem. Phys.* **1958**, *29*, 258; **1959**, *31*, 688.
(20) de Gennes, P.-G. *J. Chem. Phys.* **1971**, *55*, 572.
(21) Doi, M.; Edwards, S. F. *J. Chem. Soc., Faraday Trans 2*, **1978**, *74*, 1789.
(22) de Gennes, P.-G. "Scaling Concepts in Polymer Physics"; Cornell University Press: Ithaca, NY, 1979.
(23) The error bars on the temperature scale designate variation of temperature in the time scale where $R(q)$'s were measured from the plot of ln $I(q,t)$ vs. t.
(24) The maximum in the plot of $R(q)$ vs. q was not very sharp for every system studied here, and hence uncertainly in determing q_m directly from the plot of $R(q)$ was about the same as that in determining q_m from the plot of $R(q)/q^2$ vs. q^2. The straight lines in the plots of $R(q)/q^2$ vs. q^2 were drawn by using information of q_m's obtained from the plots of $R(q)$ vs. q.
(25) The de Gennes scaling formula of $\Lambda(q) \sim q^2$ at large q regime ($qR_0 \gg 1$)[18] was wrong as he admitted. The correction which was made by Pincus[26] suggested that $\Lambda(q) \sim q^{-2}$ at the large q regime. However, our light scattering data are obviously associated with fluctuations occurring at a distance scale much larger than the coil size, hence satisfying $qR_0 \ll 1$. Consequently, our discussions have nothing to do with the correction put forward by Pincus, and eq IV-2 and IV-8 are correct for the small q regime.
(26) Pincus, P. *J. Chem. Phys.* **1981**, *75*, 1996.
(27) It should be noted that in our previous paper[13] the constant given by eq IV-6 was erroneously neglected but the final formula of eq IV-8 is still correct.
(28) One may note that the experimental data fit with the relations, q_m^2, D_{app}, and $R(q_m)^{1/2} \sim \Delta T$ for the narrow temperature range covered in this work. However, this observation itself does not necessarily exclude other power laws such as $R(q_m)^{0.66} \sim \Delta T$, since this relation fits equally well with the data.